Wind Tunnel Characterization of a NACA 0016 Airfoil

Trevor Burgoyne, AEM 4602W, Lab Group 3Bi

16 October 2022

Abstract

This report details the experiments performed using a NACA 0016 airfoil in a Closed Return wind tunnel at Re = $3.8 \times 10^5 \pm 1.1 \times 10^4$, and the subsequent analysis performed to characterize said airfoil. The areas investigated include how C_L and C_D change at different angles of attack, as well as how velocity varies in the airfoil wake at different angles of attack and at different vertical stations behind the trailing edge. Candidates for stall angle are outlined, and results are compared to theory as well as relevant literature, with substantial agreement overall. Further investigation into this and other airfoils using similar methodology is recommended to confirm and expand upon the conclusions drawn.

Introduction

Wind tunnel experiments with airfoils have long been used to determine airfoil performance so as to inform decisions about their potential applications. When selecting an airfoil design to use for a particular project, a wind tunnel test is often performed to measure different airfoil properties and then compare them to design requirements. With near infinite variety in potential airfoil shapes and sizes, the pressing need for this kind of analysis becomes quite obvious.

To accomplish a useful characterization, several non-dimensionalized properties are calculated using the relevant measurements. The coefficients of lift (C_L) and drag (C_D), are two such values, which are defined as the ratio of force (F_L or F_D, respectively) to the product of the freestream dynamic pressure (q), which itself equal to half of the product of air density (ρ) and the square of the freestream velocity (v), and the wing area (S), where S is the product of the chord (c) and the wing span (b) for a rectangular wing.

$$q = \frac{1}{2}\rho v^2 \quad S = cb \quad C_L = \frac{F_L}{qS} \quad C_D = \frac{F_D}{qS}$$

By calculating C_L and C_D at various angles of attack (α), the angle of stall can be observed as the angle at which the otherwise linear relationship between α and C_L breaks down and begins to invert. To enable comparison of the general freestream conditions between experiments, other non-dimensional properties can be used, such as the Reynolds number (Re), which is the ratio of the product of ρ, v, and c to the dynamic viscosity (μ).

$$Re = \frac{\rho v c}{\mu}$$

Another area of interest is the wake profile that develops behind an airfoil. To acquire such measurements, care must be taken that the data collection method can distinguish between very small changes in wind speed, as well as being able to physically traverse the vertical length of the test area. Traditional ways of measuring air speed, such as a pitot tube, don't fit this particular application, and so the use of a hot wire is often much more practical, as was the case in this experiment. A hot wire takes advantage of the convective heat transfer that occurs when air moves over a heated wire. This change in temperature can trivially be interpreted as a change in voltage, and this results in a highly sensitive and mobile apparatus for measuring

airspeed. To translate the voltage (E) into an actual velocity (v), King's Law is used. This necessitates substantial calibration, and ultimately requires a linear regression to determine arbitrary constants (A), (B) and (n) used in the King's Law equation below. The method used to perform this calibration is detailed in the Results and Appendix sections.

$$E^2 = A + Bv^n$$

The wind tunnel experiment described hereafter aims to characterize the lift and drag coefficients of a NACA 0016 airfoil over a wide range of angles of attack. The lift-curve slope will be estimated and compared to relevant literature, and a likely candidate for stall angle will be discussed. Additionally, the turbulence profile will be analyzed in the airfoil wake at several angles of attack, with the intent of confirming observed behavior with existing data and related theory.

Apparatus & Methodology

The experiment was performed using a single NACA 0016 airfoil in a Closed Return (CR) wind tunnel. The airfoil was mounted to a sting which could pitch up and down to adjust the angle of attack. The angle of attack, as well as the axial and normal forces, were measured by the sting during the experiment and automatically recorded using a lab computer. The same computer received air data, such as air speed and pressure, reported from a pitot tube mounted inside the tunnel. A hot wire was suspended from the top of the tunnel and positioned behind the trailing edge of the airfoil which was capable of moving perpendicular to the freestream. The instantaneous voltage at different vertical positions within the tunnel was recorded and sent to the computer.

The experiment began with calibration of the hot wire, which was accomplished by running the wind tunnel at various speeds while keeping the hot wire at a fixed position. The data collected was later used to determine a line of best fit using King's law, which will be explained in more detail in the Results section. Once these hot wire voltages were recorded, the functionality of the sting was verified. This was accomplished by weighing the airfoil on a scale external to the wind tunnel, and then comparing the resulting weight to the forces reported by the sting once the airfoil was attached. The chord length and span of the airfoil were measured using a ruler for future calculations. With the airfoil mounted in the wind tunnel, the hot wire was positioned at a fixed distance behind the trailing edge of the airfoil, and that distance was recorded.

With the relevant equipment calibrated and in place, the experiment proceeded in two parts, with the wind tunnel always being set to the same power setting. First, multiple angles of attack were swept while measuring the forces reported by the sting. The sting was positioned at the desired angle, and then the wind tunnel was powered on. Once up to speed, the average force measurements from the sting were collected, and the tunnel was then brought back to rest before testing a new angle of attack. After successfully recording data at the desired angles, attention was turned to the hot wire voltage measurements at a smaller subset of angles of attack. Once again, the sting was set to an angle and the tunnel was brought up to speed. Then, the hot wire was positioned vertically at various stations, with the intention of capturing voltages

at representative points throughout the wake of the airfoil. Once the whole profile was characterized, the tunnel was turned off and the process began again at a different angle.

To simplify calculations, and because the airfoil spanned nearly the whole width of the tunnel, all 3D effects are ignored in this analysis. Because the freestream velocity was always well below Mach 0.3, the flow will also be considered to be incompressible, allowing for more confidence in our pitot measurements, which are in part dependent on Bernoulli's equation, which is only valid for incompressible flows. For converting the hot wire voltages into velocities, it is necessary to assume that the whole of the change in voltage is due to the freestream flow, which is fair to assume since the magnitude of any ambient heat loss will be very small in comparison. Additionally, the air temperature, density, and dynamic viscosity will be taken as constant, since the tunnel can be considered a closed system and experienced very little variation over the course of the experiment.

Uncertainty in measured quantities is considered throughout the analysis. Depending on the source, the value of uncertainty is taken from the instrument specification or derived based on the level of precision of the measurement device. The results of error propagation are included in the Results section, with the relevant calculations included in the Appendix. Table 1 below describes the uncertainties used for all the directly measured quantities in the experiment.

Sting		**Hot Wire**	
Description	**Value**	**Description**	**Value**
Forces	± 0.1 N	Position	± 1/16 in
Angle of Attack	± 0.2°		
Pitot Tube		**Airfoil**	
Wind speed	± 0.4 m/s	Chord length	± 1 mm
Air density	± 2%	Wind span	± 1 mm
Air viscosity	± 1%	Mass	± 0.5 g

Table 1: Uncertainty for various measured values.

Although not much characterization of this type has been performed with a NACA 0016 airfoil, NACA itself has conducted many similar experiments over the years that include analysis of comparable geometries, for example the report published by Jacobs et al. in 1933 [1], where the NACA 0015 and 0018 airfoils were both investigated among many others. Figures included in that report, which show lift and drag profiles at Re of 3.15×10^6, detail a region of linear lift-curve slope for low angles of attack, which breaks down at a critical point. Due to its very similar geometry, it is fair to assume that the NACA 0016 airfoil would demonstrate similar shaped lift and drag curves, just with lower overall magnitudes, since a smaller Re of $3.8 \times 10^5 \pm 1.1 \times 10^4$

was used in this experiment. The data in [1] suggests that the stall angle for similar airfoils would be at around α = 20°.

In terms of the wake profile analysis, Goodman et al. [2] provides several insightful figures that instructed how this experiment was designed. Although the data in [2] was collected at Re of $6.8x10^4$ and used a cambered airfoil, the general shape of the graphs depicting y/L_0 versus v/v_∞ and v_{rms}/v_∞ show that while the average velocity (v) *decreases* to as low as 20% of the freestream within the wake, the fluctuation in speed (v_{rms}) *increases* within the same region. Since a larger Re was used in the measurements taken in this report, it was expected that a smaller wake profile would be observed, as the inverse relationship between Re and wake size is shown by Yarusevych and Boutilier [3]. At higher Re, the flow has more forward momentum and so the wake is more uniform behind the trailing edge, with a smaller region of disturbance relative to the freestream velocity. Based on these considerations, in this experiment it was expected that, within the airfoil wake, the hot wire velocity would decrease until reaching a minimum at the center of the turbulent region, and then increase back up to the freestream speed. By contrast, the v_{rms} would follow the inverse pattern over the same exact region of investigation.

Results

Lift/Drag Experiments

From the data collected from both the sting and the pitot tube at various angles of attack, both C_D and C_L were calculated in MATLAB and are shown in Figures 1 and 2, respectively. The selection of the angles of attack seen in these figures was motivated by a desire to capture both the region of linear correlation between C_L and α as well as where that correlation breaks down into stall. Thus α was only swept by steps of 5° between -5° and 10° since a stable, linear trend was expected, whereas smaller, more frequent steps were taken between 10° and 20° so as to better identify potential candidates for the stall angle.

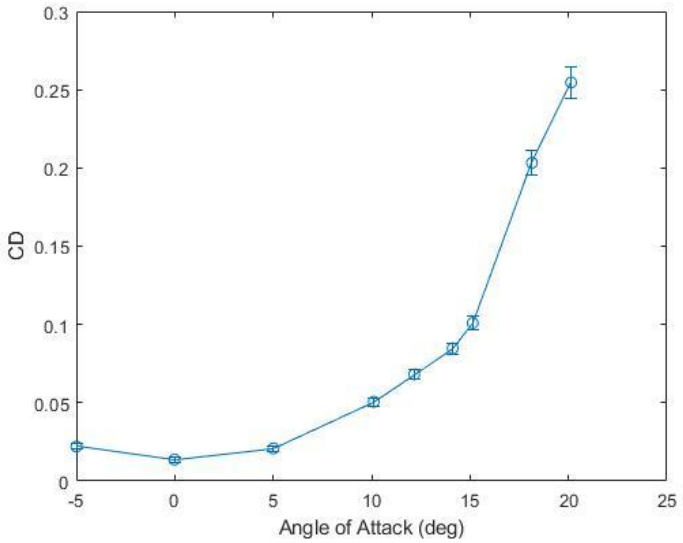

Figure 1: Drag coefficient (C_D) vs Angle of Attack (α). Measurements were taken at α = -5, 0, 5, 10, 12, 14, 15, 18, and 20 degrees. Re = $3.8x10^5 \pm 1.1x10^4$.

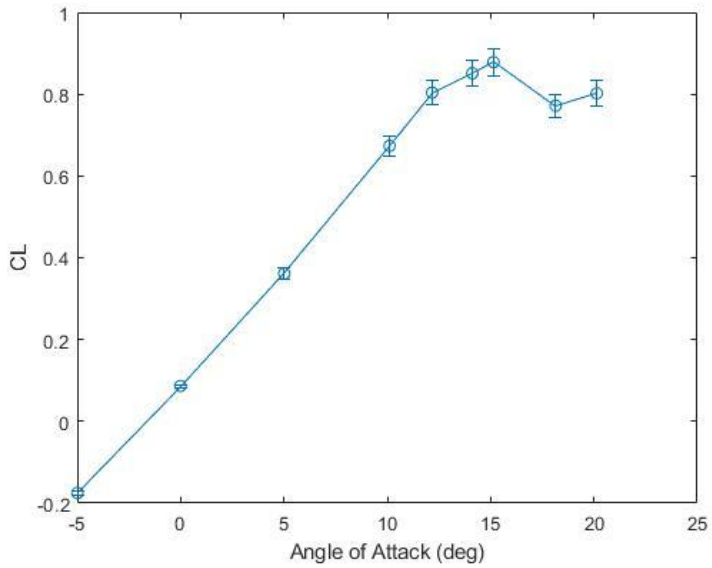

Figure 2: Lift coefficient (C_L) vs Angle of Attack (α). Measurements were taken at α = -5, 0, 5, 10, 12, 14, 15, 18, and 20 degrees. Re = $3.8x10^5$ ± $1.1x10^4$.

In Figure 1, C_D follows a somewhat linear increase from α = 0° to α = 15°, which is consistent from what is expected from airfoil theory as well as what is found in literature. For α = -5°, C_D is very similar to C_D at α = 5°, which differs from what we see happen with C_L in Figure 2. This is due to the fact that drag will always be positive, while lift can be negative for a symmetric airfoil at a negative angle of attack.

A large jump in C_D is observed at α = 18° in Figure 1, which indicates that stall likely began to occur within the range of α = 15° to α = 18°. This is supported by the sudden decrease in C_L observed in Figure 2 and the same angle. A decrease in lift and an increase in drag is precisely what is expected to occur when the boundary layer separates from the airfoil in stall.

Hot Wire Calibration

The calibration of the hot wire, as discussed in Apparatus & Methodology, was performed using King's Law and linear regression. Since the hot wire voltage readings are very sensitive to changes in airspeed, 1000 points were taken at a frequency of 100 Hz and later averaged together to provide a representative velocity calculation. Seven different airspeeds were chosen by gradually increasing the power setting on the wind tunnel by 5% at a time from 25% to 55%, which corresponded to wind speeds of about 10 m/s to 25 m/s. This spread of speeds was chosen because all experiments were to be performed at the 55% power setting, and the flow crossing the hotwire was unlikely to be slowed down by more than 60%, as evidenced by the v/v_∞ Figure 7b and c in [2], which show minimum speeds that are 40% slower than the freestream. Additionally, voltages were recorded when the wind tunnel was at rest, and that was used to inform the offset applied to all future readings.

The calculations used to generate the graph depicted in Figure 3 are included in the Appendix. The zero-velocity offset voltage was found to be -8.92 V, and values of n = 0.45, 0.5, and 0.55 were tried, with n = 0.55 ultimately providing the best fit of all, which is shown in Figure 3.

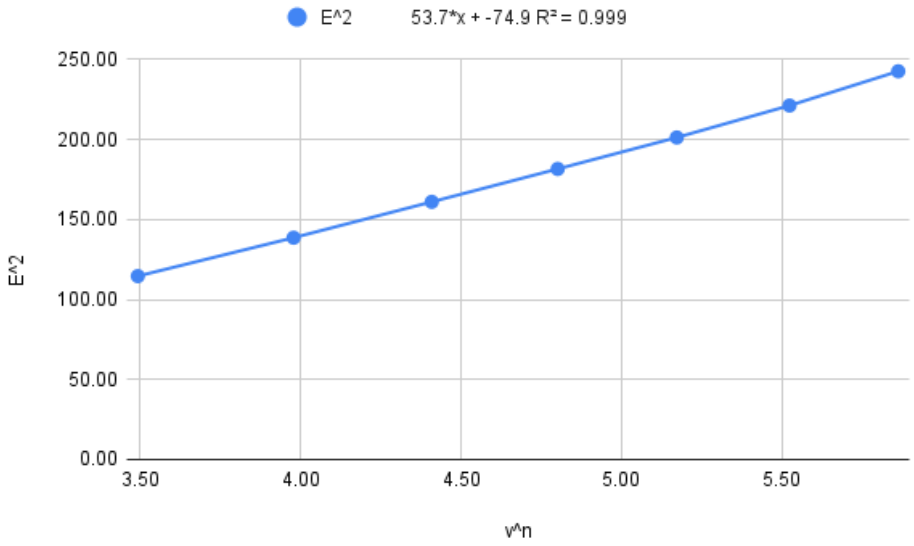

Figure 3: King's Law curve, with voltage (E) squared vs velocity (v) to the n power. The resulting linear relationship is printed above the graph in the format of Bx + A, where B = 53.7 and A = -74.9.

Using the linear regression equation from Figure 3, the relevant coefficients are listed in Table 2, in addition to the RMSE value and the aforementioned offset voltage.

Offset	n	A	B	RMSE
-8.92 V	0.55	-74.9	53.7	± 0.20 m/s

Table 2: Coefficients and values taken from the hot wire calibration. RMSE refers to the Root Mean Sum Error, whose definition is detailed in the Appendix.

The values in Table 2 can were used to provide velocity (v) as a function of hot wire voltage (E) according to King's Law, where:

$$(E + offset)^2 = A + Bx^n \leftrightarrow v(E) = \left[\frac{(E + offset)^2 - A}{B}\right]^{1/n} \pm RMSE$$

Hot Wire Wake Profile Measurements

With the hot wire calibrated, the voltages recorded at various angles of attack and at varying vertical stations behind the airfoil were converted into wake velocities, as shown in Figure 4. The vertical position (y) of the hot wire was normalized by the position (L_0) of the airfoil trailing

edge, while the air speed (v) at a given station was normalized by the freestream velocity (v_∞). More details pertaining to how y and L_0 were determined is presented in the Appendix.

Initially, the intention was to collect hot wire data for at least five different angles of attack: α = -5°, 0°, 5°, 15°, and 20°. However, due to time constraints, α = 15° was skipped in favor of α = 20°, since it was more certain that α = 20° would better exhibit behavior representative of stall conditions. At each α, the y positions were chosen based on an initial visual sweep of the whole available vertical space, with note being made of where the area of highest turbulence was located. Two measurements were taken outside either end of the turbulent regime so as to capture the return to freestream conditions, and more detailed steps of about ⅛ in were taken within it. For α = -5°, 0°, and 5°, this totaled to about 15 measurements each, whereas α = 20°, due to the large vertical span of its turbulence profile, was characterized using 78 individual measurements. As was the case in the hot wire calibration, 1000 samples were taken at each point at a frequency of 100 Hz, and these voltages were later converted to velocity using King's Law and then averaged into a single mean velocity per point. The results for the four angles of attack are detailed in Figure 4.

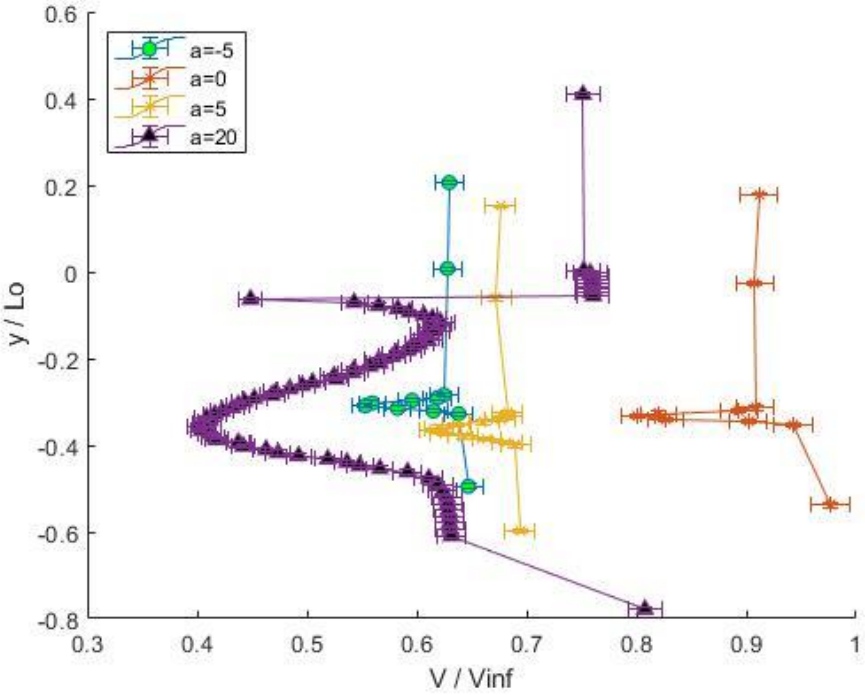

Figure 4: Hot wire position vs measured velocity, both non-dimensionalized. Four angles of attack were investigated: α = -5, 0, 5, and 20 degrees. Re = $3.8x10^5 \pm 1.1x10^4$.

In Figure 4 it can be observed that the areas of high turbulence (seen as pointy, v-shaped protrusions) occurred at relatively the same vertical position behind the airfoil, independent of angle of attack. What does change is the relative size of this turbulent region, in terms of both the y-axis and x-axis span of the peak, with the y-axis size corresponding to the vertical span of the turbulence regime and the x-axis being the magnitude of the velocities within that region. As was noted in the force analysis above, the similarities between α = -5°, and 5° agree with what

is expected of a symmetric airfoil, namely that it should behave symmetrically about α = 0°. However, it can also be noted that the noticeable difference in velocity magnitude between the two angles doesn't seem to be fully explained by the error propagation performed, so it's possible that random error or other previous unidentified sources of error had some impact on the hot wire measurements.

To further investigate the wake profile, in Figure 5 the velocity (v) is swapped out for the RMS velocity (v_{rms}), whose calculation is described in the Appendix. This provides a sense of the relative intensities of the wake profile, with higher v_{rms} corresponding to more internal variation in the velocity readings at a particular point. Instead of visualizing the average speed at each vertical station behind the trailing edge, Figure 5 depicts the magnitude of the velocity fluctuations within the 1000 samples taken at each station.

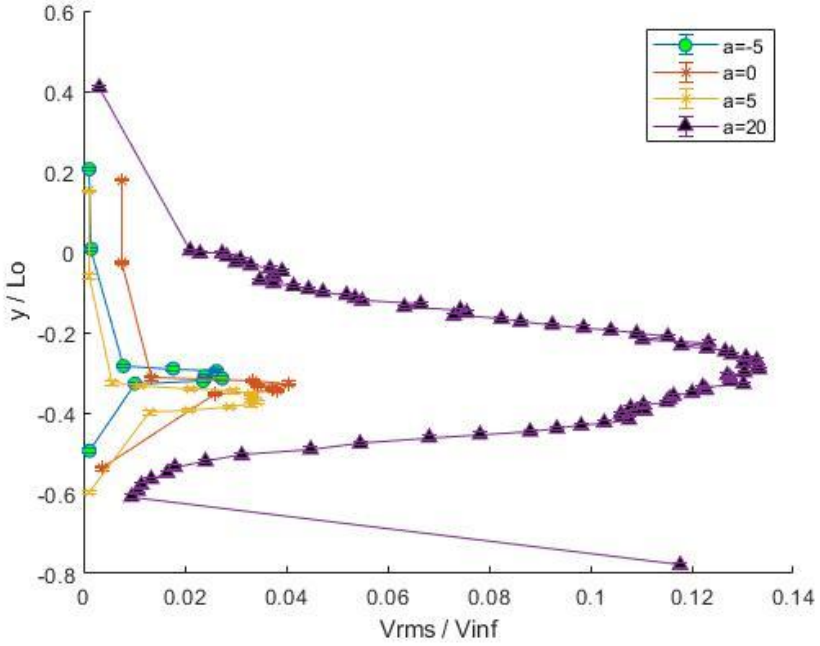

Figure 5: Hot wire position vs rms velocity, both non-dimensionalized. Four angles of attack were investigated: α = -5, 0, 5, and 20 degrees. Re = 3.8x10^5 ± 1.1x10^4.

An almost inverted trend is noted when comparing Figures 4 and 5: while at α = 20° in Figure 4 the hot wire velocities are on average much ***lower*** than at other angles, in Figure 5 it is clear that the instantaneous velocity at each station changes significantly ***more*** than at other angles. Looking more broadly, at each angle of attack, the v_{rms} peaks occur within the same y-axis range of the v peaks seen in Figure 4, meaning that they detail a trend of greater velocity fluctuation within that space in the wake. Such high variation in air speed is itself perhaps the very definition of turbulence, so this trend is precisely what one would expect to see in the airfoil wake, where flow that was previously split over the top and bottom of the wing comes crashing back together at a point behind the trailing edge.

General Discussion

From the force analysis, discussed in terms of C_D and C_L, stall was identified as occurring between α = 15° and α = 18°. Thus it is expected that angles past this range of stall should also exhibit behavior characteristic of flow after it has separated from the airfoil body, such as large magnitudes of turbulence behind the wing. This agrees nicely with the significantly exaggerated results from the wake profile analysis shown at α = 20° in Figures 4 and 5. Additionally, since a symmetric airfoil was used in the experiment, theory suggests that very little to no lift should be experienced at zero angle of attack, which once again is evidenced in both the force and hot wire analyses. In Figure 2, C_L is indeed close to zero, and in Figure 4, the α = 0° curve has by far the highest ratio of wake speed to the freestream, evidencing that the flow over the airfoil experiences the least amount of change from passing over the airfoil, as is expected in a zero-lift scenario where the pressures and speeds on the top of bottom of the airfoil are essentially equal.

These results agree well with the different sources cited earlier in this report. The NACA report from Jacobs et al. [1] details lift curves for NACA 0015 and 0018 airfoils that take a very similar shape to the ones presented here. The magnitudes of C_D and C_L are both slightly lower in this analysis, which is to be expected since measurements were taken at lower Reynolds numbers. One inconsistency that should be noted in the results shown in this report is that C_L actually increases from α = 18° to α = 20°, when the expected behavior is that C_L would continue to decrease after stall. This could mean that the data at either α = 18° or α = 20° could be erroneous, and that stall may actually occur closer to α = 20° as seen in [1]. It is an anomaly that could warrant reinvestigation.

The velocity profiles from within the airfoil wake also agree well with existing research in [2] and [3]. Goodman et al. [2] shows that while the average velocity (v) *decreases* to a minimum within the wake and then *increases* back to the freestream, the fluctuation in speed (v_{rms}) follows the exact opposite pattern within the same region. Since a larger Re was used in the measurements taken in this report, it also makes sense that smaller wake profiles than those depicted in [2] were generated, as the inverse relationship between Re and wake size is shown by Yarusevych and Boutilier [3]. One unexpected result seen in Figure 4 was the strange behavior of a few points in the α = 20° curve, which seem to spike down to a local minimum of velocity before returning to the freestream speed. This was likely due to an error in how the data was read from the files, or how it was labeled by the lab members commenting periodically in the data files. Since the group was rushed for time, any number of small errors might've been made in the data entry, but the overall trend still holds up well to comparisons with other sources.

Conclusion

The wind tunnel experiment described here aimed to characterize the lift and drag coefficients of a NACA 0016 airfoil over a wide range of angles of attack, in addition to characterizing the turbulence profile in the airfoil wake, with the intent of confirming observed behavior with existing knowledge and theory. By using measurements taken within a Closed Return wind tunnel using a force sting and hot wire, coefficients of lift and drag were calculated and the wake profile behind the airfoil body was analyzed. The stall angle for the NACA 0016 was observed to reside between α = 15° and α = 18°, and the unique characteristics of a symmetric airfoil were

confirmed, such as the angle of zero lifted being at $\alpha = 0°$ and negative and positive angles of attack producing equivalent magnitudes of lift, drag, and wake turbulence. It was also confirmed that the magnitude of the turbulence profile, both in terms of vertical size as well as the intensity of the velocity fluctuations, increased as angle of attack moved away from $\alpha = 0°$, with that increase accelerating under stall conditions.

Due to time restrictions, potentially insightful data points were passed over in favor of ensuring that the key objectives were fulfilled. Future investigation could further narrow down the precise stall angle by collecting force data for angles between $\alpha = 15°$ and $\alpha = 18°$. Additionally, wake profiles could be measured for more angles between $\alpha = 5°$ and $\alpha = 20°$ to better characterize the gradual expansion of the size of the turbulent region as angle of attack is increased. It might also be interesting to compare several different airfoil geometries and observe, for example, how camber affects the development of the turbulence profile.

Within other courses taught at the University of Minnesota, such as Fluid Mechanics (AEM 4201) and Aerodynamics (AEM 4202), significant time was dedicated to the investigation of boundary layers and their impact on fluid flow. In particular, the unit on airfoil theory in Aerodynamics discussed how the separation of the boundary layer from an airfoil body at relatively extreme angles of attack is what causes stall and the associated loss of lift. Additionally, the linear relationship between angle of attack and coefficient of lift for angles before stall was detailed, along with airfoil properties such as the angle of zero lift, and how symmetric airfoils differ from those with camber. The theory discussed in these courses aligns very well with the discussion in the Results section, where all of the concepts just mentioned were demonstrated in the experiment results. Even still, it was still clear that there was some amount of variation from what might be predicted from theory (for example, not *exactly* zero lift was noted at $\alpha = 0°$), so it is clear that thorough, detailed investigation into the performance of an airfoil would be of immense importance to those in industry looking to apply these theories to practical and profitable applications. As such, the repetition of this and similar experiments will be invaluable to those looking to further mankind's understanding of these topics.

References

[1] Jacobs, E.N., Ward, K.E., and Pinkerton, R.M., "The Characteristics of 78 Related Airfoil Sections from Tests in the Variable-Density Wind Tunnel," NACA Report No. 460, 1933, pp. 8-9. https://ntrs.nasa.gov/citations/19930091108

[2] Goodman, S., Gunasekaran, S. and Altman, A., "On the Near Wake Turbulent Flow Properties of the SD7003 Airfoil," AIAA 2019-0073, pp. 8-16. https://doi.org/10.2514/6.2019-0073

[3] Yarusevych, S., Boutilier, M.S.H., "Vortex shedding of an airfoil at low Reynolds numbers," AIAA Journal, Vol. 49, Issue 10, 2011, pp. 2221–2227. https://doi.org/10.2514/1.J051028

Appendix